International Journal of Heat and Mass Transfer 185 (2022) 122443

Contents lists available at ScienceDirect

International Journal of Heat and Mass Transfer

journal homepage: www.elsevier.com/locate/hmt

Temporally-adjustable radiative thermal diode based on metal-insulator phase change

Weixian Zhao, Zhan Zhu, Yiwen Fan, Wang Xi, Run Hu*, Xiaobing Luo

School of Energy and Power Engineering, Huazhong University of Science and Technology, Wuhan 430074, China

ARTICLE INFO

Article history:
Received 15 October 2021
Revised 27 November 2021
Accepted 16 December 2021

Keywords:
Thermal diode
Thermal rectification
Vanadium dioxide
Metal-insulator phase change

ABSTRACT

Thermal diode, which allows heat transfer between two terminals in one direction but blocks it in the opposite direction, has attracted extensive attention in recent years because of its potential applications in thermal management, energy systems, information processing and so on. Compared to the conductive thermal diode, the photon-based radiative thermal diode can break the performance limitations and achieve better thermal rectification effect. In this study, a temporally-adjustable radiative thermal diode consisting of vanadium dioxide (VO_2) and blackbody is proposed. Based on the metal-insulator phase change of vanadium dioxide, the thermal rectification could be modulated with time, thus enabling time-dependent heat flow control. The influence of shape factors on the thermal rectification is specifically investigated, revealing that the thermal rectification effect is positively correlated with the ratios of inner and outer radius of cylindrical and spherical radiative thermal diodes, and the thermal rectification effect of planar diode is stronger than that of cylindrical or spherical diode under the same settings. The temporally-adjustable photon-based thermal diode is demonstrated to be more powerful with large thermal rectification ratio, precise control of heat, and configuration adjustability.

1. Introduction

As one of the earliest semiconductor devices, electrical diode has become the cornerstone of modern electronic industry, which can be combined with other components to achieve rectification, signal modulation, voltage regulation and multiple other functionalities [1]. Inspired by the nature of electrical diode to regulate electric current, the manipulation of heat flow has also aroused widespread attention of researchers in the field of thermal science. In the past few years, the concept of thermal diode has been demonstrated both theoretically and experimentally [2–17], and its working mode can be interpreted as allowing heat flow between two terminals in a specific direction but blocking it in the opposite direction when the temperatures of the two terminals are reversed. Thanks to the unique property of heat flow control, this kind of unconventional thermal functional device has shown broad application prospects in thermal management [12,18], nanoscale heat transport [19–21], heat engine [22], thermal logic circuit [23,24], and information processing [25], etc.

Thermal diodes can be traced to phonon-based devices, where the thermal rectification mechanisms can be attributed to asymmetric nanostructures [26–29], nonlinear array structures [30], nonlinear lattice vibration [21,31,32], and the thermal deformation of contact interface [33], etc. However, limited by the phonon speed, nonlinear phonon-phonon interactions, and the existence of Kapitza resistances, the performances of these phonon-based thermal rectifiers are restricted [34,35]. For example, by deposition of boron nitride nanotubes, a conductive thermal diode was obtained by Chang et al., which has a low thermal rectification factor of 0.02~0.07 [36]. Tian et al. utilized reduced graphene oxide (rGO) with triangular shape to achieve asymmetric structure, and the conductive thermal diode obtained exhibited a thermal rectification factor of 0.26 [37], which is still not satisfactory enough. Alternatively, since the photon-mediated energy transport remains unchanged when approaching or away from the equilibrium, thermal diodes based on radiation can break the performance limitations of conductive devices and achieve more ideal thermal rectification effect [34]. In the last decade, radiative thermal diodes have been proposed in both near-field and far-field regimes. For example, in 2010, Otey et al. [5] proposed a planar near-field radiative thermal diode composed of SiC-3C and SiC-6H. Due to the different temperature dependence of the two media in the electromagnetic resonance, they demonstrated the radiative thermal rectification effect for the first time and obtained a maximum thermal rectification factor of 0.41. Lizuka et al. [38] investigated the effect of a dielectric coating on the performance of a planar near-field radiative thermal diode composed of SiC, and obtained a ther-

* Corresponding author.
E-mail address: hurun@hust.edu.cn (R. Hu).

https://doi.org/10.1016/j.ijheatmasstransfer.2021.122443
0017-9310/

Nomenclature

d	distance between two terminals [m]
λ_W	characteristic radiation wavelength [m]
T_1	temperature of hot terminal [K]
T_2	temperature of cold terminal [K]
T_0	mean temperature of the phase transition temperature of VO_2 [K]
q_F	forward radiative heat flux [W m^{-2}]
q_R	reverse radiative heat flux [W m^{-2}]
t	normalized time
σ	Stefan-Boltzmann constant [W m^{-2} K^{-4}]
A_1	radiant surface area of blackbody [m^2]
A_2	radiant surface area of VO_2 [m^2]
ε_F	forward effective emissivity
ε_R	reverse effective emissivity
R	thermal rectification factor
ε_1	emissivity of blackbody
ε_2	emissivity of VO_2
r_1	radius of inner cylinder/sphere [m]
r_2	radius of outer hollow cylinder/spherical shell [m]
r	radius ratio = r_1 / r_2

mal rectification factor of 0.44 by optimizing the permittivity and the thickness of the coating when the temperatures of two terminals were 500 K and 300 K, respectively. Wang et al. [15] investigated the near-field thermal rectification effect of intrinsic silicon and several other materials at different temperatures and vacuum gaps. The results showed that when the temperatures of the two terminals were 1000 K and 300 K, the thermal rectification factor of thermal diode consisting of intrinsic silicon and doped silicon with a vacuum gap of 5 nm can reach 0.73. Under the identical settings, the thermal diode made of intrinsic silicon and silicon dioxide (SiO_2) has a thermal rectification factor up to 0.91. Besides, the thermal diode composed of intrinsic silicon and gold can achieve a high thermal rectification factor of 0.85 in a wide vacuum gap of 100~500 nm. Nefzaoui et al. [39] proposed a far-field radiative thermal diode consisting of selective emitters, which were multilayer structures composed of Au/Si and HDSi/Si, respectively. They found that the thermal rectification factor increased with the increase of temperature difference of two terminals, and a thermal rectification factor of 0.19 was obtained when the temperature difference was 370 K. It can be observed that in order to achieve thermal rectification effect, the radiative thermal diodes mentioned above require extremely small gaps between two terminals or large temperature differences, which is hard to achieve in practice so far.

Vanadium dioxide (VO_2), as a typical kind of solid-solid phase change materials, has garnered lots of interest in recent years due to its special characteristic of reversible metal-insulator transition (MIT) around 340 K, which results in a temperature-dependent emissivity regulation [40]. To be specific, when the temperature is lower than 340 K, vanadium dioxide in its insulating state corresponds to a high emissivity of 0.79, while when the temperature is higher than 340 K, it will experience a transition from insulator to metal in a small temperature interval, resulting in a drop of emissivity to 0.22 [6,41,42]. This temperature-dependent change in emissivity shows great potential in radiative thermal diodes. For example, Abdallah et al. [43] proposed a planar radiative thermal diode composed of vanadium dioxide and silicon dioxide, and obtained a thermal rectification factor of more than 0.7 by taking advantage of the metal-insulator transition property of vanadium dioxide.

In this paper, we propose a temporally-adjustable radiative thermal diode, which consists of vanadium dioxide and blackbody. Based on the metal-insulator phase change of vanadium dioxide, the thermal rectification effect can be modulated with time, resulting in time-dependent heat flow control. Moreover, the corresponding numerical expressions for different types of radiative thermal diodes, namely the planar diode, the cylindrical diode and the spherical diode are derived, and the influence of shape factors on the thermal rectification effect for these different radiative thermal diodes are investigated.

2. Theoretical modeling

As illustrated in Fig. 1, the radiative thermal diode considered in this paper consists of two semi-infinite parallel plates, whose materials are vanadium dioxide (VO_2) and blackbody, respectively. The distance d between the two plates is larger than the radiation wavelength $\lambda_W(T)$ at the corresponding temperature, that is, we consider the thermal radiation in the far field condition. In the forward bias, the temperature of blackbody is T_1, and the temperature of vanadium dioxide is T_2, where T_1 remains 400 K and T_2 is a temporally-adjustable temperature function expressed as $T_2 = T_0 + \Delta T(t)$. In this temperature function, T_0 is set as the mean temperature of phase transition temperature during heating and cooling process, and $\Delta T(t)$ is defined as $\Delta T(t)=8sin(2\pi t)$. It is worth mentioning that the amplitude of sinusoidal $\Delta T(t)$ should be large enough ($\geq$ 8 K) to cover the thermal hysteresis loop of vanadium dioxide after one period. Such temperature modulation can be experimentally achieved by electrical heating or cooling devices, but it is necessary to ensure that the period of heating or cooling is shorter than the thermalization time of vanadium dioxide. Under this circumstance, the net radiative heat transfer from blackbody to vanadium dioxide is defined as the forward heat flow (q_F). In the reverse bias, the temperature conditions of the two terminals exchange with each other, in which case the net radiative heat transfer from vanadium dioxide to blackbody is defined as the reverse heat flow (q_R). With the identical settings, cylindrical and spherical thermal diodes, as shown in Fig. 2, are also considered for exploring the influence of shape factors on the thermal rectification effect. Note that r_1 is the radius of inner cylinder for cylindrical diode or the radius of inner sphere for spherical diode, and r_2 is the inside radius of outer hollow cylinder for cylindrical diode or the inside radius of outer spherical shell for spherical diode.

For thermal radiation between the two terminals with configurations shown in Fig. 1 and Fig. 2, the forward and reverse heat flow can be identified by resorting to the Stefan-Boltzmann's law:

$$q_F = \sigma A_1 \varepsilon_F \left({T_1}^4 - {T_2}^4\right) \tag{1}$$

$$q_R = \sigma A_2 \varepsilon_R \left({T_1}^4 - {T_2}^4\right) \tag{2}$$

where σ is the Stefan-Boltzmann constant, A_1 and A_2 are areas of the radiant surfaces, ε_F and ε_R are the forward effective emissivity and the reverse effective emissivity respectively, T_1 and T_2 are temperatures of the two terminals respectively. Here, we only consider the heat transfer between the two terminals without taking the interaction with environment into consideration, and thus Eq. (1) and (2) are the governing equations.

In order to evaluate the thermal rectification effect of thermal diodes, the thermal rectification factor is defined as

$$R = \frac{|q_F - q_R|}{\max(q_F,\ q_R)} \tag{3}$$

From Eq. (1) and Eq. (2), the definition of thermal rectification factor can be further simplified as

$$R = \frac{|A_1\varepsilon_F - A_2\varepsilon_R|}{\max(A_1\varepsilon_F,\ A_2\varepsilon_R)} \tag{4}$$

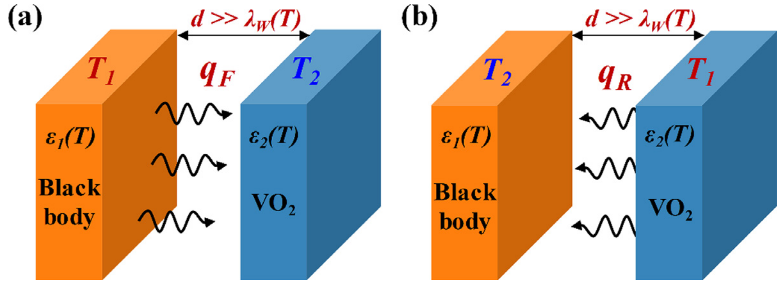

Fig. 1. (a) Forward bias of the planar diode. (b) Reverse bias of the planar diode.

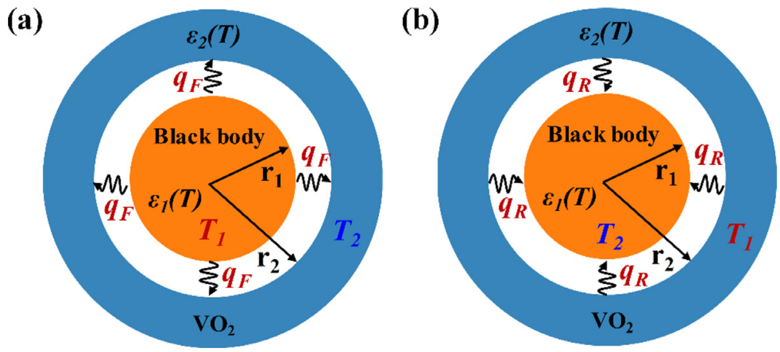

Fig. 2. (a) Forward bias of the cylindrical/spherical diode. (b) Reverse bias of the cylindrical/spherical diode.

Through this definition, it can be observed that the rectification factor is between 0 and 1, which means a higher thermal rectification factor corresponds to a better thermal rectification effect. Moreover, the thermal rectification factor depends on the effective emissivities and radiant areas, which is affected by the shapes of the radiative thermal diodes. Therefore, we will further derive the detailed parameters of planar, cylindrical and spherical radiative thermal diodes in subsequent sections.

2.1. Planar diode

For the purpose of simplicity, the planar radiative thermal diode considered here has the same radiant area at the both terminals, namely A_1=A_2. Therefore, the forward effective emissivity and the reverse effective emissivity can be obtained as follows:

$$\varepsilon_F = \left(\frac{1}{\varepsilon_1(T_1)} + \frac{1}{\varepsilon_2(T_2)} - 1\right)^{-1} \tag{5}$$

$$\varepsilon_R = \left(\frac{1}{\varepsilon_1(T_2)} + \frac{1}{\varepsilon_2(T_1)} - 1\right)^{-1} \tag{6}$$

where $\varepsilon_1(T)$ and $\varepsilon_2(T)$ represent the emissivities of blackbody and vanadium dioxide at the corresponding temperature T, respectively. Since the emissivity of blackbody equals to unity and it is independent on temperature, namely $\varepsilon_1(T) = 1$, the final form of forward and reverse effective emissivities can be written as $\varepsilon_F = \varepsilon_2(T_2)$ and $\varepsilon_R = \varepsilon_2(T_1)$, respectively. According to the derivation mentioned above, the thermal rectification factor of the planar diode can be denoted as

$$R = \frac{|\varepsilon_F \;-\; \varepsilon_R|}{\max(\varepsilon_F,\;\; \varepsilon_R)} \tag{7}$$

2.2. Cylindrical diode

As illustrated in Fig. 2, the cylindrical radiative thermal diode is composed of a cylinder and a concentric hollow cylinder, of which the inner cylinder is blackbody and the outer hollow cylinder is vanadium dioxide. The two cylinders are of the same length, thus the heat transfer between them is carried out through their profiles. In this situation, the forward effective emissivity and the reverse effective emissivity can be obtained as follows:

$$\varepsilon_F = \left(\frac{1}{\varepsilon_1(T_1)} + \left(\frac{1}{\varepsilon_2(T_2)} - 1\right) r\right)^{-1} \tag{8}$$

$$\varepsilon_R = \left(\frac{1}{r\varepsilon_1(T_2)} + \frac{1}{\varepsilon_2(T_1)} - 1\right)^{-1} \tag{9}$$

Where r is the radius ratio of the two cylinders, defined as $r = r_1/r_2$. In the same way, the thermal rectification factor of the cylindrical diode can be expressed as

$$R = \frac{|r\varepsilon_F \;-\; \varepsilon_R|}{\max(r\varepsilon_F,\;\; \varepsilon_R)} \tag{10}$$

2.3. Spherical diode

Similar to the structure of the cylindrical diode mentioned above, the spherical diode considered here consists of concentric structures composed of a sphere and a spherical shell, of which the inner sphere is blackbody and the outer spherical shell is vanadium dioxide. In this case, the radiative heat transfer is achieved through the outer surface of the sphere and the inner surface of the sphere shell. Thus, the forward effective emissivity and the reverse effective emissivity can be given by

$$\varepsilon_F = \left(\frac{1}{\varepsilon_1(T_1)} + \left(\frac{1}{\varepsilon_2(T_2)} - 1\right) r^2\right)^{-1} \tag{11}$$

$$\varepsilon_R = \left(\frac{1}{r^2\varepsilon_1(T_2)} + \frac{1}{\varepsilon_2(T_1)} - 1\right)^{-1} \tag{12}$$

Where r is the radius ratio of the sphere and the spherical shell, defined as $r = r_1/r_2$. Similarly, the thermal rectification factor of the spherical diode can be denoted as

$$R = \frac{\left|r^2\varepsilon_F \;-\; \varepsilon_R\right|}{\max\,(r\varepsilon_F,\;\; \varepsilon_R)} \tag{13}$$

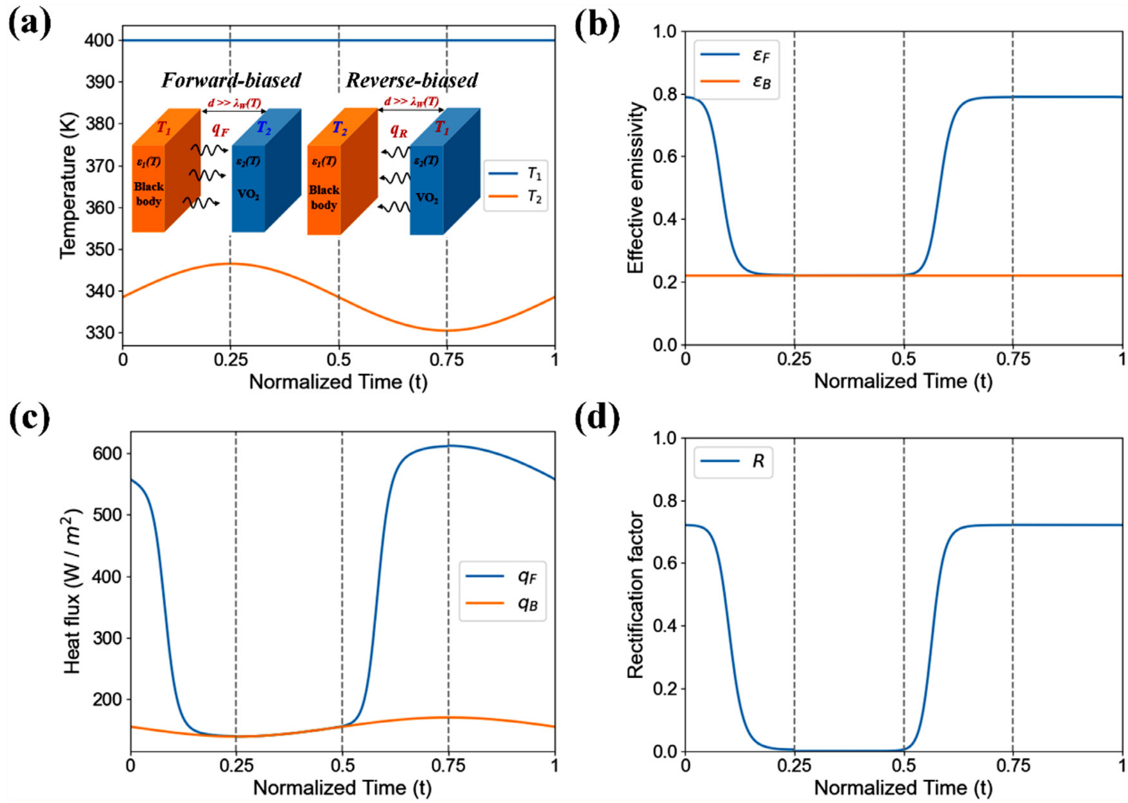

Fig. 3. (a) Temperature variation curves with time of two terminals of the planar diode. (b) The forward and reverse effective emissivities variation curves with time of the planar diode. (c) The forward and reverse heat flow curves with time of the planar diode. (d) The thermal rectification factor curves with time of the planar diode.

3. Results and discussions

According to our setup, the temperature T_1 at the hot end is fixed at 400 K, and the temperature T_2 at the cold end is the initial temperature T_0 plus a sinusoidal temperature function $\Delta T(t)=8\sin(2\pi t)$. Fig. 3(a) shows the temperature variation curves with time of the two terminals of the planar diode. When vanadium dioxide is heated or cooled near the phase transition temperature, a reversible metal-insulator transition will occur, which leads to the change of its emissivity, and further results in the change of forward and reverse effective emissivities. For planar diode, the forward and reverse effective emissivities can be written as $\varepsilon_F = \varepsilon_2(T_2)$ and $\varepsilon_R = \varepsilon_2(T_1)$, as derivations described above. As can be seen from the final form of the forward effective emissivity ε_F, it depends on the emissivity change of the vanadium dioxide with temperature T_2. In the first quarter period, the forward effective emissivity drops significantly, which can be interpreted as the emissivity decreases due to the transition from insulator to metal with the increase of T_2. When the phase transition is completed, the forward effective emissivity remains constant ($\varepsilon_F = 0.22$) for some time with the decrease of T_2, which can be explained as the thermal hysteresis effect of vanadium dioxide keeps it in a metallic state. As T_2 further decreases to the cooling phase transition temperature, vanadium dioxide transforms from metal to insulator, leading to an increase in its emissivity. In the fourth quarter period, T_2 rises and the forward effective emissivity remains constant ($\varepsilon_F = 0.79$), which can also be attributed to the existence of thermal hysteresis. Since T_1 is fixed at 400 K, in which case the vanadium dioxide is in a metallic state, so the reverse effective emissivity ε_R is a constant value independent of time, as illustrated in Fig. 3(b).

From Eq. (1) and Eq. (2), the curves of forward and reverse heat flow with time can be calculated, as shown in Fig. 3(c). It can be observed that on account of the large variation range of forward effective emissivity, the forward heat flow shows a great variation with time, which exhibits approximately the same trend as that of the forward effective emissivity. However, since the reverse effective emissivity is a constant, the reverse heat flow depends on the difference between T_1 and T_2 to the fourth power. Due to the characteristics of forward and reverse heat flow with time, the thermal rectification effect occurs when there is a difference between them, and the larger the difference, the better the thermal rectification effect, which is manifested as the larger the thermal rectification factor, as illustrated in Fig. 3(d). Note that in the middle stage of a period, the magnitude of the forward and reverse flow is equal, resulting in a thermal rectification factor of zero.

Under the same conditions, the relevant results of cylindrical radiative thermal diode are shown in Fig. 4. It can be observed that the variation trend of parameters of the cylindrical diode with time is roughly the same as that of the planar diode, as mentioned above. In order to further explore the influence of the radius ratio of the inner and outer cylinders on the thermal rectification effect, the results when radius ratio r is 0.8, 0.6, 0.4, and 0.2 are calculated. As illustrated in Fig. 4(b), the larger the radius ratio, the smaller the forward effective emissivity and the larger the reverse effective emissivity, which corresponds to the results of Eq. (8) and Eq. (9). Moreover, with the increase of radius ratio, the forward and reverse heat flow also increase, which can be explained that the radiation is determined by both the emissivity and the radiant area, that is, the radiant area under high radius ratio is larger, resulting in the larger radiative heat flow under the condition of a smaller emissivity. Note that as the radius ratio increases, the difference between the forward and reverse heat flow increases, leading to the enhancement of the thermal rectification effect, which corresponds to a larger thermal rectification factor, as shown in Fig. 4(d).

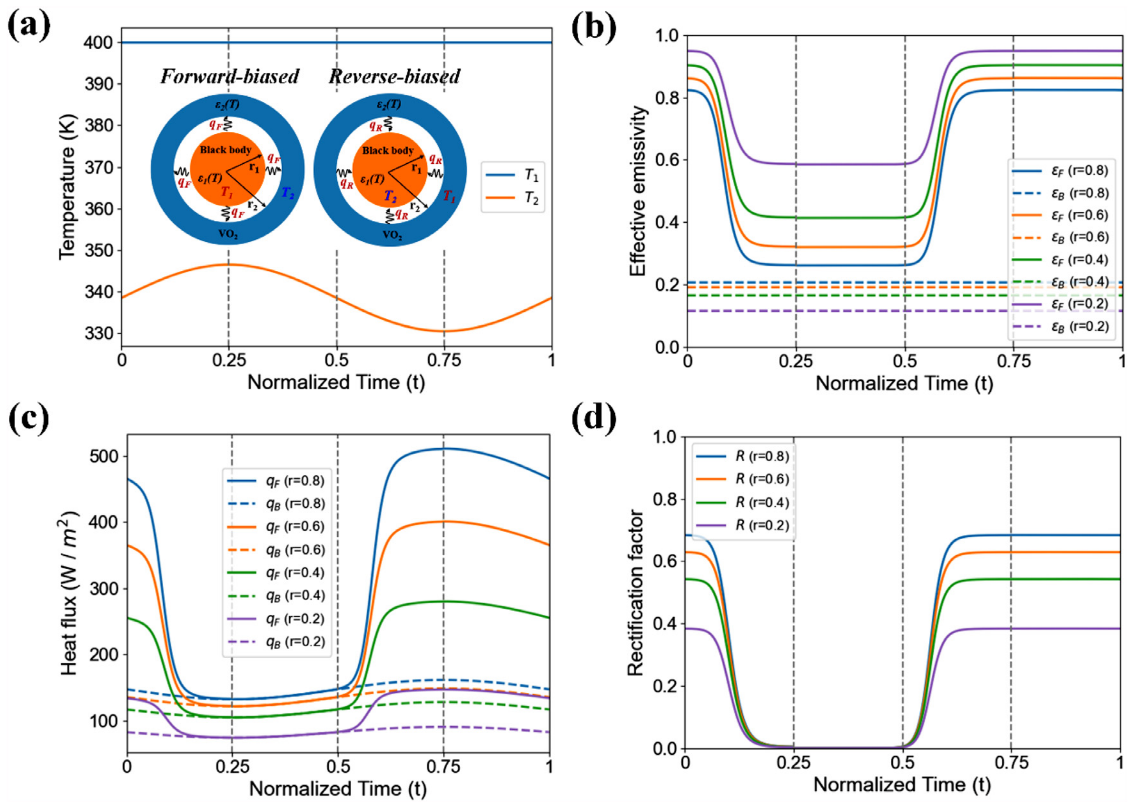

Fig. 4. (a) Temperature variation curves with time of two terminals of the cylindrical diode. (b) The forward and reverse effective emissivities variation curves with time of the cylindrical diode under different radius ratios. (c) The forward and reverse heat flow curves with time of the cylindrical diode under different radius ratios. (d) The thermal rectification factor curves with time of the cylindrical diode under different radius ratios.

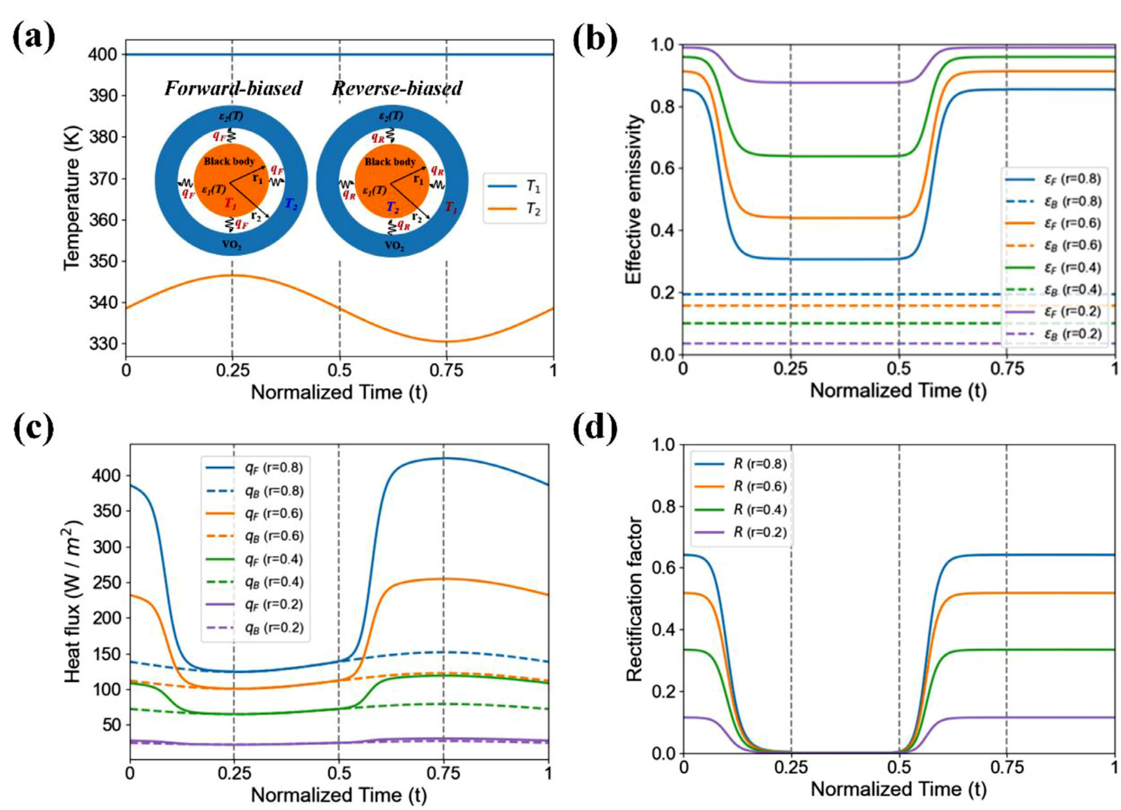

Fig. 5. (a) Temperature variation curves with time of two terminals of the spherical diode. (b) The forward and reverse effective emissivities variation curves with time of the spherical diode under different radius ratios. (c) The forward and reverse heat flow curves with time of the spherical diode under different radius ratios. (d) The thermal rectification factor curves with time of the spherical diode under different radius ratios.

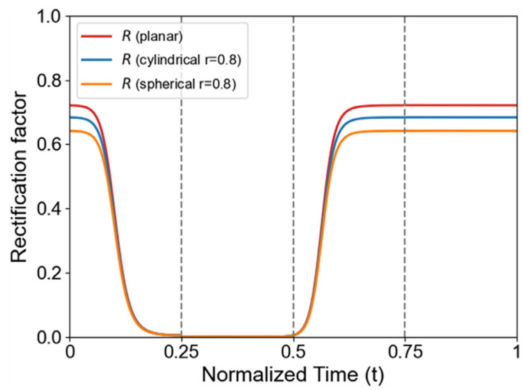

Fig. 6. Comparison of thermal rectification factors of planar, cylindrical and spherical diodes.

The results of spherical radiative thermal diode are shown in Fig. 5. It can be found that the variation of parameters is consistent with that of planar and cylindrical diodes. To investigate the influence of radius ratio of the inner sphere and the outer spherical shell on the thermal rectification effect, the results when radius ratio r is 0.8, 0.6, 0.4, and 0.2 are also calculated. As can be seen from Fig. 5(b), with the increase of radius ratio, the forward effective emissivity decreases and the reverse effective emissivity increases. Moreover, at the same radius ratio, the forward effective emissivity of spherical diode is lager and its reverse effective emissivity is smaller than that of the cylindrical diode, which corresponds to the Eq. (11) and Eq. (12). The forward and reverse heat flow are shown in Fig. 5(c). It can be observed that when the radius ratio is small, such as $r = 0.2$, the curves of forward and reverse heat flow are almost coincident, which indicates that the thermal rectification effect is weak in this situation. However, as the radius ratio increases, the difference between forward and reverse heat flow increases gradually, resulting in a larger thermal rectification factor, as illustrated in Fig. 5(d).

As discussed above, for cylindrical and spherical radiative thermal diodes, the higher radius ratio provides better thermal rectification effect. In order to explore the influence of shape factors on the thermal rectification effect, the comparison of thermal rectification factors of planar, cylindrical and spherical diodes is shown in Fig. 6. It is observed that the planar diode can achieve the best thermal rectification effect, whose maximum thermal rectification factor is 0.72, higher than the value of 0.68 of cylindrical diode and the value of 0.64 of spherical diode. The results mentioned above have proven the temporally-adjustable characteristic of the radiative thermal diode and the optimization design of thermal rectification effect carried out by the shape factors.

4. Conclusion

In conclusion, we propose a temporally-adjustable radiative thermal diode consisting of vanadium dioxide (VO_2) and black body. Based on the metal-insulator phase transition of vanadium dioxide (VO_2), the thermal rectification effect with time regulating property is achieved. To explore the influence of shape factors on the thermal rectification effect, we derive the numerical expressions of planar, cylindrical and spherical radiative thermal diodes and carry out the calculations. The obtained results indicate that the thermal rectification effect is positively correlated with the ratios of inner and outer radius of cylindrical and spherical diodes, which means lager ratio of inner and outer radius leads to higher thermal rectification factor. Moreover, under the same settings, it can be observed that the thermal rectification effect of planar diode is stronger than that of cylindrical diode or spherical diode. The results of this paper provide the possibility of time modulation of radiative thermal diode and are instructive to optimize the thermal rectification effect by shape factors.

Declaration of Competing Interest

The authors declare that they have no known competing financial interests or personal relationships that could have appeared to influence the work reported in this paper.

Acknowledgements

The authors acknowledge the financial support from the National Natural Science Foundation of China (52076087), Wuhan City Science and Technology Program (2020010601012197).

CRediT authorship contribution statement

Weixian Zhao: Conceptualization, Methodology, Investigation, Writing – original draft. **Zhan Zhu:** Data curation, Investigation, Methodology. **Yiwen Fan:** Validation, Discussion. **Wang Xi:** Writing – review & editing. **Run Hu:** Conceptualization, Supervision, Writing – review & editing, Funding acquisition. **Xiaobing Luo:** Writing – review & editing.

References

[1] N. Li, J. Ren, L. Wang, G. Zhang, P. Hänggi, B. Li, Colloquium: phononics: manipulating heat flow with electronic analogs and beyond, Rev. Mod. Phys. 84 (2012) 1045–1066.
[2] S. Basu, M. Francoeur, Near-field radiative transfer based thermal rectification using doped silicon, Appl. Phys. Lett. 98 (2011) 113106.
[3] A. Fiorino, D. Thompson, L. Zhu, R. Mittapally, S.A. Biehs, O. Bezencenet, N. El-Bondry, S. Bansropun, P. Ben-Abdallah, E. Meyhofer, P. Reddy, A thermal diode based on nanoscale thermal radiation, ACS Nano 12 (2018) 5774–5779.
[4] A. Ghanekar, J. Ji, Y. Zheng, High-rectification near-field thermal diode using phase change periodic nanostructure, Appl. Phys. Lett. 109 (2016) 123106.
[5] S. Huang, J. Zhang, M. Wang, R. Hu, X. Luo, Macroscale thermal diode-like black box with high transient rectificaion ratio, ES Energy Environ. 6 (2019) 51–56.
[6] R. Hu, S. Huang, M. Wang, L. Zhou, X. Peng, X. Luo, Binary thermal encoding by energy shielding and harvesting units, Phys. Rev. Appl. 10 (2018) 054032.
[7] W. Gu, G. Tang, W. Tao, Thermal switch and thermal rectification enabled by near-field radiative heat transfer between three slabs, Int. J. Heat Mass Tran. 82 (2015) 429–434.
[8] J. Huang, Q. Li, Z. Zheng, Y. Xuan, Thermal rectification based on thermochromic materials, Int. J. Heat Mass Tran. 67 (2013) 575–580.
[9] K. Joulain, Y. Ezzahri, J. Drevillon, B. Rousseau, D. De Sousa Meneses, Radiative thermal rectification between SiC and SiO2, Opt. Express 23 (2015) A1388–A1397.
[10] W. Kobayashi, D. Sawaki, T. Omura, T. Katsufuji, Y. Moritomo, I. Terasaki, Thermal rectification in the vicinity of a structural phase transition, Appl. Phys. Express 5 (2012) 027302.
[11] E. Pallecchi, Z. Chen, G.E. Fernandes, Y. Wan, J.H. Kim, J. Xu, A thermal diode and novel implementation in a phase-change material, Mater. Horiz. 2 (2015) 125–129.
[12] A. Pugsley, A. Zacharopoulos, J.Deb Mondol, M. Smyth, Theoretical and experimental analysis of a horizontal planar Liquid-Vapour Thermal Diode (PLVTD), Int. J. Heat Mass Tran. 144 (2019) 118660.
[13] J. Shen, X. Liu, H. He, W. Wu, B. Liu, High-performance noncontact thermal diode via asymmetric nanostructures, J. Quant. Spectrosc. Ra. 211 (2018) 1–8.
[14] G. Xing, W. Zhao, R. Hu, X. Luo, Spatiotemporal modulation of thermal emission from thermal-hysteresis vanadium dioxide for multuplexing thermotronics functionalities, Chin. Phys. Lett. 38 (2021) 124401.
[15] L.P. Wang, Z.M. Zhang, Thermal rectification enabled by near-field radiative heat transfer between intrinsic silicon and a dissimilar material, Nanosc. Microsc. Therm. 17 (2013) 337–348.
[16] Y. Yang, S. Basu, L. Wang, Radiation-based near-field thermal rectification with phase transition materials, Appl. Phys. Lett. 103 (2013) 163101.
[17] Y. Yang, S. Basu, L. Wang, Vacuum thermal switch made of phase transition materials considering thin film and substrate effects, J. Quant. Spectrosc. Ra. 158 (2015) 69–77.
[18] T. Villeneuve, M. Boudreau, G. Dumas, The thermal diode and insulating potentials of a vertical stack of parallelogrammic air-filled enclosures, Int. J. Heat Mass Tran. 108 (2017) 2060–2071.
[19] O. Ilic, N.H. Thomas, T. Christensen, M.C. Sherrott, M. Soljacic, A.J. Minnich, O.D. Miller, H.A. Atwater, Active radiative thermal switching with graphene plasmon resonators, ACS Nano 12 (2018) 2474–2481.
[20] B. Li, L. Wang, G. Casati, Thermal diode: rectification of heat flux, Phys. Rev. Lett. 93 (2004) 184301.

[21] C.R. Otey, W.T. Lau, S. Fan, Thermal rectification through vacuum, Phys. Rev. Lett. 104 (2010) 154301.
[22] N.A. Roberts, D.G. Walker, A review of thermal rectification observations and models in solid materials, Int. J. Therm. Sci. 50 (2011) 648–662.
[23] L. Wang, B. Li, Thermal logic gates: computation with phonons, Phys. Rev. Lett. 99 (2007) 177208.
[24] L. Wang, B. Li, Phononics gets hot, Phys. World 21 (2008) 27–29.
[25] T. Ruokola, T. Ojanen, A.P. Jauho, Thermal rectification in nonlinear quantum circuits, Phys. Rev. B 79 (2009) 144306.
[26] Y. Wang, A. Vallabhaneni, J. Hu, B. Qiu, Y.P. Chen, X. Ruan, Phonon lateral confinement enables thermal rectification in asymmetric single-material nanostructures, Nano Lett 14 (2014) 592–596.
[27] P. Kim, L. Shi, A. Majumdar, P.L. McEuen, Thermal transport measurements of individual multiwalled nanotubes, Phys. Rev. Lett. 87 (2001) 215502.
[28] C.W. Chang, D. Okawa, H. Garcia, A. Majumdar, A. Zettl, Nanotube phonon waveguide, Phys. Rev. Lett. 99 (2007) 045901.
[29] C.W. Chang, D. Okawa, H. Garcia, A. Majumdar, A. Zettl, Breakdown of Fourier's law in nanotube thermal conductors, Phys. Rev. Lett. 101 (2008) 075903.
[30] A. Arora, T. Hori, T. Shiga, J. Shiomi, Thermal rectification in restructured graphene with locally modulated temperature dependence of thermal conductivity, Phys. Rev. B 96 (2017) 165419.
[31] M. Terraneo, M. Peyrard, G. Casati, Controlling the energy flow in nonlinear lattices: a model for a thermal rectifier, Phys. Rev. Lett. 88 (2002) 094302.
[32] B. Hu, L. Yang, Y. Zhang, Asymmetric heat conduction in nonlinear lattices, Phys. Rev. Lett. 97 (2006) 124302.
[33] Y. Li, X. Shen, Z. Wu, J. Huang, Y. Chen, Y. Ni, J. Huang, Temperature-dependent transformation thermotics: from switchable thermal cloaks to macroscopic thermal diodes, Phys. Rev. Lett. 115 (2015) 195503.
[34] P. Ben-Abdallah, S.A. Biehs, Contactless heat flux control with photonic devices, AIP Adv 5 (2015) 053502.
[35] P. Ben-Abdallah, S.A. Biehs, Near-field thermal transistor, Phys. Rev. Lett. 112 (2014) 044301.
[36] C.W. Chang, D. Okawa, A. Majumdar, A. Zettl, Solid-state thermal rectifier, Science 314 (2006) 1121.
[37] H. Tian, D. Xie, Y. Yang, T. Ren, G. Zhang, Y. Wang, C. Zhou, P. Peng, L. Wang, L. Liu, A novel solid-state thermal rectifier based on reduced graphene oxide, Sci. Rep. 2 (2012) 1–7.
[38] H. Iizuka, S. Fan, Rectification of evanescent heat transfer between dielectric–coated and uncoated silicon carbide plates, J. Appl. Phys. 112 (2012) 024304.
[39] E. Nefzaoui, J. Drevillon, Y. Ezzahri, K. Joulain, Simple far-field radiative thermal rectifier using Fabry-Perot cavities based infrared selective emitters, Appl. Opt. 53 (2014) 3479–3485.
[40] M.A. Kats, R. Blanchard, S. Zhang, P. Genevet, C. Ko, S. Ramanathan, F. Capasso, Vanadium dioxide as a natural disordered metamaterial: perfect thermal emission and large broadband negative differential thermal emittance, Phys. Rev. X 3 (2013) 041004.
[41] J. Ordonez-Miranda, Y. Ezzahri, J.A. Tiburcio-Moreno, K. Joulain, J. Drevillon, Radiative thermal memristor, Phys. Rev. Lett. 123 (2019) 025901.
[42] M.M. Qazilbash, M. Bresh, B.G. Chae, P.C. Ho, G.O. Andreev, B.J. Kim, S.J. Yun, A.V. Balatsky, M.B. Maple, F. Keilmann, H.T. Kim, D.N. Basov, Science 318 (2007) 1750–1753.
[43] P. Ben-Abdallah, S.A. Biehs, Phase-change radiative thermal diode, Appl. Phys. Lett. 103 (2013) 191907.